Nonrelativistic Dirac equation: An application to photoionization of highly charged hydrogenlike ions

Tor Kjellsson Lindblom, Simen Bræck, and Sølve Selstø*
Department of Computer Science, Oslo Metropolitan University, NO-0130 Oslo, Norway

(Received 11 September 2024; accepted 10 December 2024; published 26 December 2024)

We investigate the role of relativity in photoionization of hydrogenlike ions by a laser pulse. For hydrogen, the wavelengths of the laser resides in the weakly ultraviolet region. For higher nuclear charges, the laser parameters are scaled in a manner which renders the time-dependent Schrödinger equation in the electric dipole approximation independent of nuclear charge. The ionization potentials of these highly charged ions are strongly modified by relativistic effects. In an earlier work by Ivanova *et al.* [Phys. Rev. A **98**, 063402 (2018)], it is demonstrated how this explains most of the relativistic correction to the ionization probability. Here we investigate to what extent remaining discrepancies can be attributed to relativistic effects stemming from the strong external field. To this end, we solve semirelativistic formulations of both the Schrödinger and the Dirac equations; the former accounts for increased inertia due to the external laser field, while the latter features a nonrelativistic interaction term.

DOI: 10.1103/PhysRevA.110.063120

I. INTRODUCTION

Motivated by experimental breakthroughs, we have seen an increased interest in the theoretical and computational study of relativistic dynamics for atoms and ions exposed to strong laser pulses [1]. Such investigations tend to be quite demanding from a computational point of view as the ionization process is governed by the time-dependent Dirac equation, which typically is quite hard to solve. For this reason, many studies resort to models and approximations—such as the *strong-field approximation* and models of reduced dimensionality. However, also on the theoretical and computational side we have seen recent breakthroughs when it comes to fully relativistic descriptions (see, e.g., Refs. [2–13]). Specifically, in Refs. [11,12] a promising technique coined the *generalized pseudospectral method* is applied. Reference [8], in which the Klein-Gordon equation is solved numerically, is particularly interesting as it provides a direct comparison between relativistic calculations in full dimensionality with both analytical approximations and numerical calculations performed within a two-dimensional model. Moreover, it has also been shown how exponential speedup in solving the Dirac equation may be achieved on a quantum computer [14].

The numerical solution of the time-dependent Dirac equation is subject to several issues which its nonrelativistic counterpart, the time-dependent Schrödinger equation, does not suffer from. For instance, many conventional numerical schemes for the time evolution are subject to very restrictive limitations on the numerical time step. This problem may, however, often be evaded by the use of so-called Magnus propagators [15].

Another issue, which arises when using spectral methods, is the fact that the inclusion of the spatial dependence of external electromagnetic fields, such as laser pulses, is nontrivial [6,16]. While the full spatial dependence has been incorporated in relativistic calculations (see, e.g., Refs. [4,11,12]), it has been shown that this challenge to a large extent can be overcome at a low computational cost by formulating the interaction in what is coined the *propagation gauge* [7,17–20]. Yet another fruitful approach is that of expanding the external field in terms of a finite Fourier series [13]. Also, within a nonrelativistic framework, the notion of *partial Fourier transforms* within a split operator scheme [21,22] seems a promising venue—one that hopefully can be extended into the relativistic realm in the near future.

Other methods aim to incorporate relativistic corrections in a nonrelativistic context by means of a semirelativistic Schrödinger equation. Substituting the electron's rest mass with a field-dressed, relativistic mass has proven to be a viable path in this direction [9]. For strong fields, this approach has been used to describe photoionization of atoms at photon energies in both the optical [23] and the x-ray [20,24] regime—in addition to ultraviolet frequencies with general ellipticity [25]. Incidentally, it has also been shown that a similar mass replacement may be introduced into a nonrelativistic framework in order to account for the mass shift induced by internal energy transitions for a moving atom [26].

In Ref. [27] the photoionization of various hydrogenlike ions by laser pulses was studied in a relativistic framework. For hydrogen, the photon energies involved corresponded to the weakly ultraviolet region—more specifically, with wavelengths ranging from 100 to about 400 nm. For highly charged ions, with the laser parameters scaled accordingly, strong relativistic effects were seen in the total ionization yield. It was convincingly argued that these corrections predominantly originated from relativistic corrections to the ionization potential of the ions as the nuclear charge Z was increased. To this end, another set of approximate scaling relations was

*Contact author: solvese@oslomet.no

introduced which, to a large extent, was able to reproduce the ionization probabilities obtained for the nonrelativistic hydrogen case, $Z = 1$.

These relativistic calculations were performed within the so-called electric dipole approximation, in which the spatial dependence of the vector potential corresponding to the external laser field is neglected. For reasons we will return to, the scaling of the laser parameters renders the dipole approximation questionable for higher nuclear charges Z. Still, the argument that the increased ionization potential should lead to shifted, reduced ionization probability should hold. However, the shift of the spectrum of the unperturbed ion does not explain the relativistic photoionization yield in full. By direct solutions of the Schrödinger equation and the Dirac equation—within and without semirelativistic approximations—we set out to identify potential relativistic corrections induced by the external field adding to relativistic effects stemming from the strong Coulomb attraction from the nucleus.

The paper is organized as follows: In Sec. II the theoretical framework and numerical implementations are outlined, and in Sec. III the results are presented and discussed. Conclusions are drawn in Sec. IV. Expressions are generally given using SI units. However, some quantities are given in atomic units, in which case this is stated explicitly.

II. THEORY AND IMPLEMENTATION

The time-dependent Dirac equation may, like its nonrelativistic counterpart, the Schrödinger equation, be written

$$i\hbar\frac{d}{dt}\Psi = H\Psi. \tag{1}$$

The wave function Ψ is a scalar function in the Schrödinger equation, while the state is a four-component vector in the Dirac case. The relativistic Hamiltonian H^{R} is a 4×4 matrix:

$$H^{\mathrm{R}} = c\boldsymbol{\alpha}\cdot(\mathbf{p}+e\mathbf{A}) + V(r;Z)\,I_4 + mc^2\beta. \tag{2}$$

Here,

$$V(r;Z) = -\frac{1}{4\pi\varepsilon_0}\frac{Z}{r} \tag{3}$$

is the Coulomb potential of the nucleus, which is assumed to be of infinite mass. We have here applied the minimal coupling or the so-called velocity gauge form of the interaction, while, for the α matrices, we have adopted the usual formulation in terms of Pauli matrices:

$$\alpha_k = \begin{pmatrix} 0 & \sigma_k \\ \sigma_k & 0 \end{pmatrix}, \tag{4}$$

where k is either x, y, or z, and

$$\beta = \begin{pmatrix} I_2 & 0 \\ 0 & -I_2 \end{pmatrix}. \tag{5}$$

The velocity gauge form of the nonrelativistic Schrödinger Hamiltonian reads

$$H^{\mathrm{NR}} = \frac{(\mathbf{p}+e\mathbf{A})^2}{2m} + V(r;Z) \tag{6a}$$

$$H_0^{\mathrm{NR}} + \frac{e}{m}\mathbf{A}\cdot\mathbf{p} + \frac{e^2}{2m}\mathbf{A}^2, \tag{6b}$$

where H_0^{NR} is the time-independent part of the nonrelativistic Schrödinger Hamiltonian.

The external laser pulse enters via the vector potential $\mathbf{A}$. In our numerical studies, we impose the electric dipole approximation, i.e., we will take $\mathbf{A}$ to be purely time dependent. Consequently, the electric field will be homogeneous and the magnetic field will be absent. This approximation is valid for sufficiently weak and short pulses when the extension of the atom is considerably smaller than the photon wavelength. Although, in our case, this assumption is less justified for higher nuclear charges, this does not prevent us from illustrating how the alternative, semirelativistic formulations of the interaction enable us to distinguish between structural and dynamical relativistic effects.

A. Relativistic mass in the Schrödinger equation

In Ref. [9] it is explained how relativistic corrections induced by the external field $\mathbf{A}$ may be accounted for within the Schrödinger equation by replacing the rest mass m by the field-dressed effective mass. In that paper, this is done via the relativistic version of the propagation gauge [7]. This way of formulating the interaction, which was first introduced in a nonrelativistic context [18,19], is provided by a gauge transformation to a frame in which the electron momentum follows that of a classical electron in the direction of the light propagation. This motivates its name. It has proven to be numerically favorable to more conventional ways of formulating the interaction in various regimes.

As we here, as mentioned, will apply the electric dipole approximation, the formalism simplifies a bit. Specifically, the expression for the field-dressed mass reads

$$\mu(t) = m\sqrt{1+\left(\frac{e\mathbf{A}}{mc}\right)^2}. \tag{7}$$

As in the general case, also the dipole form of the semirelativistic Hamiltonian can be derived from the Dirac equation. However, neglecting spin and relativistic corrections to the Coulomb potential, it may also conveniently be obtained directly from the Hamiltonian function

$$H = \sqrt{m^2c^2 + (\mathbf{p}+e\mathbf{A})^2} - mc^2 + V(r;Z). \tag{8}$$

By introducing the relativistic mass, Eq. (7), and truncating the square-root expression at first order,

$$\begin{aligned} c\sqrt{m^2c^2 + (\mathbf{p}+e\mathbf{A})^2} &= c\sqrt{\mu^2c^2 + (\mathbf{p}^2 + 2e\mathbf{A}\cdot\mathbf{p})} \\ &\approx \mu c^2\left(1 + \frac{1}{2\mu^2c^2}(\mathbf{p}^2 + 2e\mathbf{A}\cdot\mathbf{p})\right), \end{aligned} \tag{9}$$

we obtain the mass-adjusted semirelativistic Hamiltonian as an almost direct replacement of m by $\mu(t)$ in Eq. (6a):

$$H_{\mathrm{S}}^{\mathrm{SR}} = \frac{\mathbf{p}^2}{2\mu(t)} + \frac{e}{\mu(t)}\mathbf{A}\cdot\mathbf{p} + \frac{e^2}{2m}\mathbf{A}^2 + V(r;Z) \tag{10a}$$

$$H_0^{\mathrm{NR}} + \left(\frac{1}{\mu(t)} - \frac{1}{m}\right)\frac{\mathbf{p}^2}{2} + \frac{e}{\mu(t)}\mathbf{A}\cdot\mathbf{p} + \frac{e^2}{2m}\mathbf{A}^2. \tag{10b}$$

Note that the correction to the kinetic-energy term in effect introduces an additional interaction term as compared to Eq. (6b).

The notion of a field-dressed, effective mass enables us to account for strong-field relativistic effects induced by the external field accelerating the electron towards a significant fraction of the speed of light. Correspondingly, a comparison of the solutions of the Schrödinger equation with the Hamiltonians of Eqs. (6) and (10) should reveal such effects.

B. Nonrelativistic interaction in the Dirac equation

If we separate the Hamiltonian of Eq. (2) in a time-dependent and a time-independent part, it reads

$$H^{\mathrm{R}} = H_0^{\mathrm{R}} + c\boldsymbol{\alpha}\cdot\mathbf{A}. \tag{11}$$

In Ref. [16] an alternative, nonrelativistic form of the interaction was presented. For completeness, we will here briefly revise the derivation of this formulation, which is attributable to Lindroth.

By introducing the Foldy-Wouthuysen-like unitary transformation [28]

$$\Psi' = U\Psi \quad \text{with} \quad U = \exp\left[\frac{e}{2mc}\beta\boldsymbol{\alpha}\cdot\mathbf{A}\right], \tag{12}$$

and formulating the Dirac equation, Eq. (1), in terms of Ψ' rather than Ψ, we arrive at the effective Hamiltonian

$$H_{\mathrm{D}}^{\mathrm{SR}} = UH^{\mathrm{R}}U^{\dagger} + i\hbar\frac{\partial U}{\partial t}U^{\dagger}. \tag{13}$$

If we expand U up to second order, we will find that $H_{\mathrm{D}}^{\mathrm{SR}}$ may be written

$$H_{\mathrm{D}}^{\mathrm{SR}} = c\boldsymbol{\alpha}\cdot\mathbf{p} + \frac{e}{m}\mathbf{A}\cdot\mathbf{p}\,\beta + \frac{e^2}{2m}A^2\,\beta + \frac{e\hbar}{2m}\boldsymbol{\sigma}\cdot\mathbf{B}\,\beta + V(r;Z) + O(c^{-2}), \tag{14}$$

which holds beyond the dipole approximation as well. In arriving at Eq. (14), we impose the Coulomb gauge restriction: $\nabla\cdot\mathbf{A} = 0$. Also, the identity

$$(\boldsymbol{\alpha}\cdot\mathbf{a})(\boldsymbol{\alpha}\cdot\mathbf{b}) = \mathbf{a}\cdot\mathbf{b} + i\boldsymbol{\sigma}\cdot(\mathbf{a}\times\mathbf{b}) \tag{15}$$

is useful in deriving this semiclassical form of the interaction.

Within the dipole approximation, the magnetic field $\mathbf{B} = \nabla\times\mathbf{A}$ vanishes, and we arrive at the following semirelativistic formulation:

$$H_{\mathrm{D}}^{\mathrm{SR}} = c\boldsymbol{\alpha}\cdot\mathbf{p} + \left(\frac{e}{m}\mathbf{A}\cdot\mathbf{p} + \frac{e^2}{2m}\mathbf{A}^2\right)\beta + V(r;Z) \tag{16a}$$

$$= H_0^{\mathrm{R}} + \left(\frac{e}{m}\mathbf{A}\cdot\mathbf{p} + \frac{e^2}{2m}\mathbf{A}^2\right)\beta. \tag{16b}$$

Equation (16) is semiclassical in the sense that it features the interaction terms of the nonrelativistic Schrödinger Hamiltonian within the minimal coupling formulation. Apart from the β matrix, the interaction terms of Eq. (16b) coincide with those of Eq. (6b).

The crucial difference between Eqs. (16b) and (6b) is their time-independent parts, H_0. In the former case, this part is fully relativistic and, thus, entirely capable of resolving the relativistic structure of the system. Relativistic effects induced by the external laser field, on the other hand, are *not* resolved by this formulation as it features a nonrelativistic formulation of the interaction. Correspondingly, by comparing the predictions within the two different formulations of the Dirac Hamiltonian, we should be able to distinguish between structural and dynamical relativistic effects—between relativistic corrections induced, respectively, by the Coulomb interaction alone on one hand and the external laser field—or the interaction between the two—on the other.

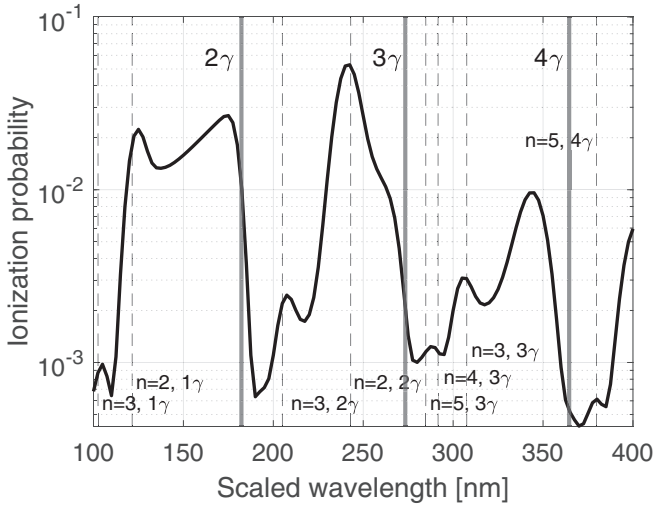

FIG. 1. The ionization probability for a hydrogenlike ion as a function of the scaled wavelength $\tilde{\lambda}$ obtained using the fully nonrelativistic Hamiltonian of Eqs. (6). The scaled maximum field strength is $\tilde{E}_0 = 0.03$ a.u., which corresponds to an intensity of $3.16\times10^{13}\,\mathrm{W/cm^2}$ for hydrogen. The thick gray vertical lines correspond, from left to right, to the onset of the two, three, and four photon ionization thresholds. The dashed lines are the wavelengths corresponding to resonant intermediate bound states. Their principal quantum number n and the corresponding number of photons absorbed in the resonant transition are indicated in the figure.

C. Scaling relations

It has been shown that, by introducing the appropriate scaling of the variables and laser parameters, the time-dependent Schrödinger equation for the laser-matter interaction becomes independent of the nuclear charge within the dipole approximation [29]. We will identify these scaled variables and parameters by a tilde:

$$\tilde{r} = Zr, \tag{17a}$$

$$\tilde{t} = Z^2 t, \tag{17b}$$

$$\tilde{E}_0 = E_0/Z^3, \tag{17c}$$

$$\tilde{\omega} = \omega/Z^2. \tag{17d}$$

As an illustration, we demonstrate the ionization probability as a function of the scaled wavelength $\tilde{\lambda} = \lambda/Z^2$ in Fig. 1. For a hydrogen atom, the wavelength falls into the moderately ultraviolet region. To the extent that the dipole approximation and the nonrelativistic treatment are valid, this plot is independent of Z. Here, the scaled peak intensity is $\tilde{I} = 3.16\times10^{13}\,\mathrm{W/cm^2}$. According to Eq. (17c), the actual peak intensity $I = Z^6\tilde{I}$.

As explained in Refs. [27,30], the strongly nonmonotonic behavior is due to the onset of the two-, three-, and four-photon thresholds, accompanied by pronounced peaks where photon absorption happens to be in resonance with intermediate excited bound states [resonantly enhanced multiphoton ionization (REMPI)]. The ionization probability is seen to increase considerably when such transitions involving intermediate states are energetically admissible, indicated by dashed vertical lines. The thicker vertical lines indicate the multiphoton thresholds. The overall ionization probability features a dramatic drop when the photon wavelength increases beyond these thresholds and an additional photon is required to reach the continuum. We also see a tendency for the ionization probability, including the height of the REMPI peaks, to increase as the wavelength increases towards these thresholds.

As mentioned, the Z independence does not survive any transition beyond the dipole approximation or to any relativistic description. Thus, any deviation from the scaling law of Eqs. (17) is indicative of the breakdown of the dipole approximation and/or the nonrelativistic approach—the latter in the present case. Specifically, since the extension of the atom, according to Eqs. (17), scales as Z^{-1} while the photon wavelength $\lambda = 2\pi c/\omega$ scales as Z^{-2}, their ratio is proportional to Z, thus indicating the breakdown of the validity of the dipole approximation as the nuclear charge increases. In the ultraviolet region, this breakdown is confirmed in Ref. [12].

It is worth repeating that in Ref. [27] another set of approximate scaling relations which also accounted for the relativistic shift in ionization potential was imposed. These scaling relations were quite successful in explaining the photoionization's dependence of laser wavelength within the dipole approximation. In this context, however, we will resort to the scaling of Eqs. (17).

D. Implementation

A spectral method is applied for resolving the time evolution dictated by Eq. (1). The wave functions are expressed in terms of basis functions consisting of the eigenstates of the time-independent part of the Hamiltonians, $H_0^{\mathrm{R/NR}}$, by means of expansions in B-splines [31] and spherical harmonics. Specifically, for the time-independent Dirac Hamiltonian, the basis functions have the form

$$\psi^{\mathrm{R}}_{n,\kappa,m_j} = \frac{1}{r}\begin{pmatrix} P_{n,\kappa}(r)X_{j,m_j,\kappa}(\Omega) \\ iQ_{n,\kappa}(r)X_{j,m_j,-\kappa}(\Omega)\end{pmatrix}, \tag{18a}$$

$$P_{n,\kappa}(r) = \sum_i a^i_{n,\kappa} B^{k_1}_i(r), \tag{18b}$$

$$Q_{n,\kappa}(r) = \sum_i b^i_{n,\kappa} B^{k_2}_i(r), \tag{18c}$$

$$X_{\kappa,m_j}(\Omega) = \sum_{m_\ell,m_s} \langle \ell, m_\ell, 1/2, m_s | j, m_j\rangle \chi_{m_s} Y_{\ell,m_\ell}(\Omega), \tag{18d}$$

$$\kappa = \begin{cases} \ell, & j = \ell - 1/2 \\ -(\ell+1), & j = \ell + 1/2 \end{cases}, \tag{18e}$$

where $B^k_i(r)$ is a B-spline of order k and χ_{m_s} is an eigenspinor. We impose Dirichlet boundary conditions at $r_{\max} = 250/Z$ a.u.

The nonrelativistic basis functions are simpler:

$$\psi^{\mathrm{NR}}_{n,\ell,m_\ell} = \frac{1}{r} P_{n,\ell}(r) Y_{\ell,m_\ell}(\Omega), \tag{19}$$

where the radial part $P_{n,\ell}(r)$ is expanded analogously to Eq. (18b).

For linearly polarized fields pointing along the z axis described within the dipole approximation, we need only include angular components within the same m quantum number, be it m_j or m_ℓ, as the initial ground state. We include all angular momenta ℓ up to $\ell_{\max} = 20$, as well as all states with energies below $mc^2 + Z^2\times 100$ a.u. for the positive part of the spectrum and above $-mc^2 - Z^2\times 100$ a.u. for the negative part; prior works have shown that the negative part of the spectrum cannot be neglected in general (see, e.g., Refs. [16,30]). The numerical solution of the time-independent Dirac equation is typically plagued with the emergence of so-called spurious states. For the present method, Ref. [32] has presented detailed evidence that the choice $k_1 = k_2 \pm 1$ for the order or the B-splines used to expand $P_{n,\kappa}$ and $Q_{n,\kappa}$ in Eqs. (18b) and (18b), respectively, successfully resolves this issue. Here, we have chosen the values $k_1 = 7$ and $k_2 = 8$, which, in our experience provide good accuracy for these kinds of calculations [6,7].

For a Coulomb potential strong enough to induce relativistic effects, a uniform knot sequence is highly impractical in solving the time-independent Dirac equation. Instead we have applied the same type of sequence as in Ref. [30]: the knot points are first distributed in a geometric sequence which switches to a linear distribution at a certain point. We found that $N_{\mathrm{knot}} = 759$ with geometric factor 1.05 and switching point at the 280th knot point gives well-converged good numerical spectra for the relativistic calculations in this paper.

For the solution of the time-dependent Dirac equations, we need to calculate coupling elements of the form

$$\langle \psi^{\mathrm{R}}_{n,\kappa,m_j} | H_I | \psi^{\mathrm{R}}_{n',\kappa',m'_j}\rangle, \tag{20}$$

where H_I would correspond to α_z in the case of Eq. (11) and $p_z\beta$ and β, respectively, in the case of Eq. (16). Each of these coupling elements is to be multiplied with their appropriate time-dependent factor. The corresponding nonrelativistic matrix element,

$$\langle \psi^{\mathrm{NR}}_{n,\ell,m_\ell} | H_I | \psi^{\mathrm{NR}}_{n',\ell',m'_\ell}\rangle, \tag{21}$$

has $H_I \sim p_z$ for the Hamiltonian of Eq. (6b) and $\mathbf{p}^2$ and p_z, respectively, for Eq. (10b). In both cases, the term proportional to $\mathbf{A}^2$ may safely be ignored since this is a purely time-dependent factor in the dipole approximation. The radial integrals involved in calculating the coupling elements of Eqs. (20) and (21) are evaluated by a Gauss-Legendre quadrature.

Next, the time evolution is carried out by propagating the state vector using a Magnus-type propagator [15]:

$$\Psi(t+\tau) \approx \exp[-i/\hbar\, H(t+\tau/2)\tau]\Psi(t) + O(\tau^3). \tag{22}$$

This evades the extreme restriction that the numerical time step must be significantly lower than the inverse of the electron's mass energy, which several other propagation schemes suffer from when solving the time-dependent Dirac equation. On the other hand, repeatedly exponentiating large matrices is not tractable either. To this end, we have approximated the action of the Magnus propagator in Eq. (22) by projecting it into the time-dependent Krylov subspace of dimension k,

$$\exp[-i/\hbar\, H(t+\tau/2)\tau]\Psi(t) \approx V \exp[-i/\hbar\, H_{\mathcal{K}}(t+\tau/2)\tau]V^{\dagger}\Psi(t), \tag{23}$$

where the orthonormal Krylov basis consists of the columns of the projection matrix V. These, in turn, are constructed from the set obtained from the repeated series of matrix-vector multiplications

$$[H(t+\tau/2)]^m\Psi(t), \quad m=0,\ldots,k-1 \tag{24}$$

by the Arnoldi procedure with reorthogonalization. The Krylov representation of the Hamiltonian matrix, $H_{\mathcal{K}}$, is a $k\times k$ matrix, where k is considerably lower than the full dimensionality of the numerical problem. Thus, the most time consuming part is not the exponentiation but rather the repeated series of matrix-vector multiplications, Eq. (24). These iterations are performed until the estimated error of the propagated wave is below some specified limit [33].

For all cases presented here we have checked for convergence in all numerical parameters. It is found that 450–600 numerical time steps per optical cycle suffices for the Krylov propagators to converge within $k=15$ iterations for the nonrelativistic calculations and 30 iterations for the relativistic ones per time step. The factor 2 in the relativistic Krylov subspace size is directly related to the stiffness induced by the mass energy term, i.e., the last term in the Hamiltonian of Eq. (2). For the Dirac equation our predictions were compared with the corresponding results of Ref. [27] and found to be in agreement.

III. RESULTS AND DISCUSSION

As mentioned, we take our laser field to be linearly polarized along the z axis. Moreover, we use a model for the homogeneous laser pulse of this shape:

$$A(t) = \frac{E_0}{\omega}\,\sin^2\left(\frac{\pi}{T}t\right)\sin(\omega t), \quad t\in[0,T]. \tag{25}$$

The pulse duration corresponds to 20 optical cycles. Although the dipole approximation, as mentioned, may be challenged for the systems at hand, our calculations should still enable us to distinguish relativistic effects induced by the Coulomb field alone from those stemming from the external laser field.

For the hydrogen case, no noticeable difference between nonrelativistic, semirelativistic, or fully relativistic calculations is seen. For higher nuclear charges, however, we see strong deviations between the predictions of the Schrödinger equation and the Dirac equation. Figure 2 shows the relativistic ionization probability for the same case as in Fig. 1 with $Z=50$ and 92. Although the laser intensity is somewhat higher than the one applied in Ref. [27], what we see is in perfect alignment with the findings of that paper: the ionization probability is shifted towards lower wavelengths and

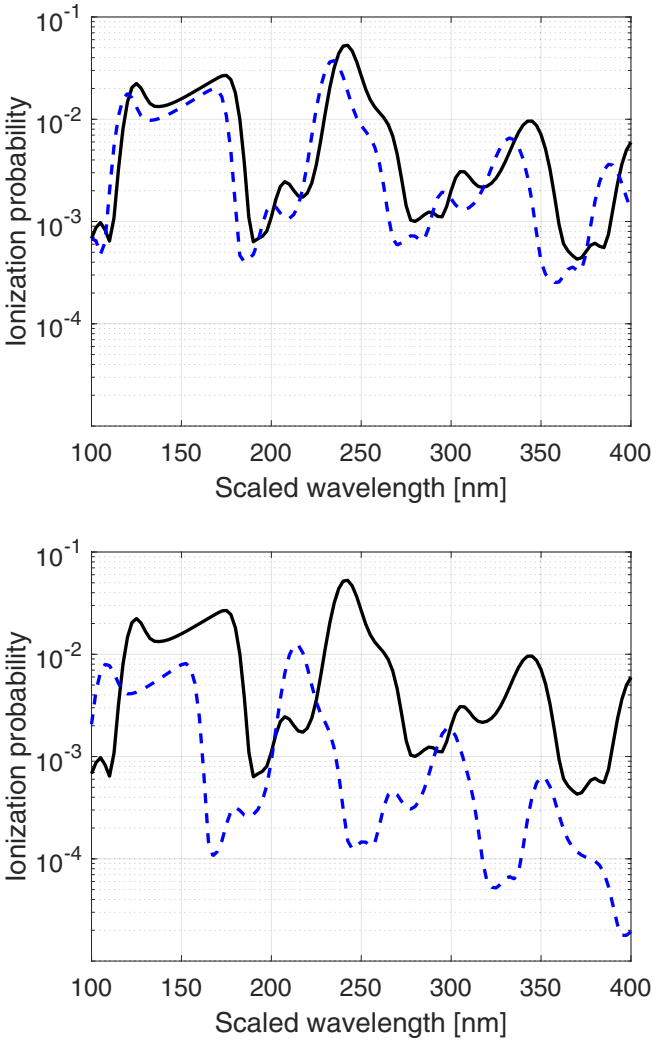

FIG. 2. The ionization probability for a hydrogenlike ion with nuclear charge $Z=50$ (upper) and $Z=92$ (lower). The scaled field parameters are the same as in Fig. 1. The black curve is the Z-independent prediction from the Schrödinger equation within the dipole approximation while the blue dashed curve is obtained solving the full Dirac equation within the dipole approximation.

there is an overall downshift in ionization yield. The former was convincingly explained in terms of increased ionization potential. To some extent, this relativistic shift can also, via the introduction of an effective nuclear charge, explain the decrease in overall yield, but not fully.

To investigate this further, we have solved the semirelativistic Schrödinger equation, i.e., we have solved Eq. (1) using the Hamiltonian of Eq. (10). While this will not be able to explain the shift towards lower wavelengths, one may hope that the decrease in ionization yield can be understood in terms of increased inertia induced by the laser pulse. The results are shown in Fig. 3 for the same cases as in Fig. 2.

As it turns out, introducing the relativistic mass has actually led to an *increase* of the ionization yield. This may appear surprising since the replacement $m\to\mu(t)$, in effect, reduces the strength of the laser field in the dipole interaction term:

$$\frac{e}{m}\mathbf{A}\cdot\mathbf{p} \to \frac{e}{m}\mathbf{A}_{\rm eff}\cdot\mathbf{p} \quad \text{with} \quad \mathbf{A}_{\rm eff}(t) = \frac{m}{\mu(t)}\mathbf{A}(t). \tag{26}$$

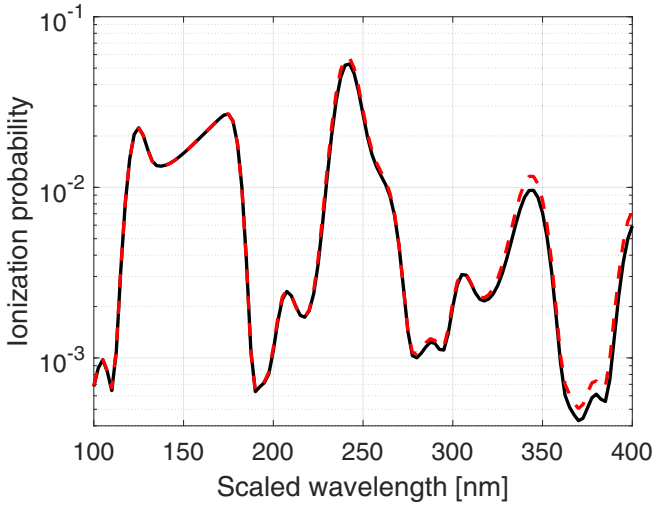

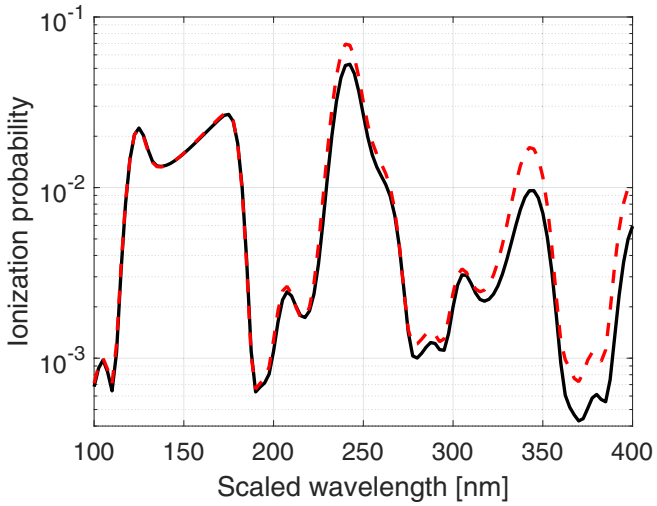

FIG. 3. The ionization probability for a hydrogenlike ion with nuclear charge $Z = 50$ (upper) and $Z = 92$ (lower). The scaled field parameters are the same as in Figs. 1 and 2. As before, the black curve is the result from the Schrödinger equation, while the red dashed curve is obtained using the semirelativistic Schrödinger Hamiltonian of Eq. (10).

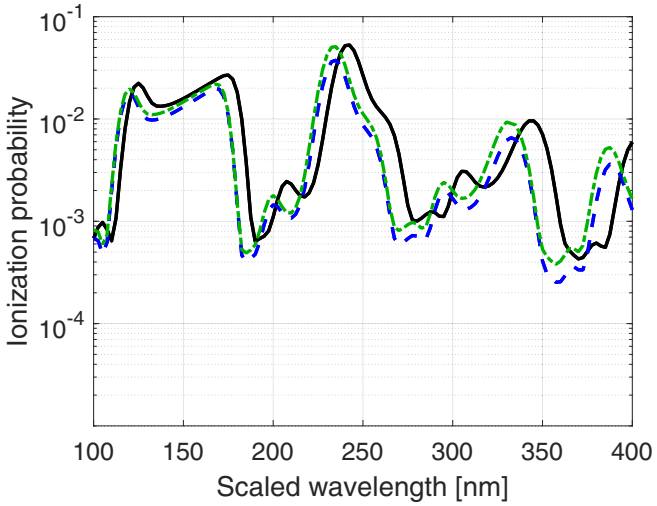

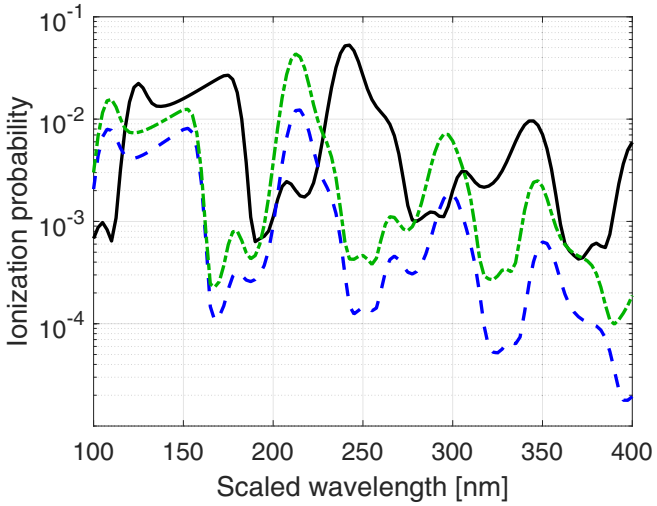

FIG. 4. Same as Fig. 2 with the additional inclusion of results obtained with the semirelativistic Dirac Hamiltonian in Eq. (16) (green dash-dotted curves).

However, as also the kinetic-energy term is affected by the field-dressed mass, a second ionization mechanism is introduced [see Eq. (10b)]. Apparently, this mechanism compensates any decrease that comes about via the reduced effective field strength for the cases at hand.

Next, we implement the other semirelativistic approach—the one in which the time-independent part remains fully relativistic, Eq. (16). The resulting ionization probability is shown in Fig. 4. With a fully relativistic spectrum for the unperturbed system, it should come as no surprise that the shift towards lower wavelengths is reproduced. More interestingly, the Dirac Hamiltonian with nonrelativistic interaction overestimates the ionization yield.

Despite the conclusion in regard to Fig. 3, we will still argue that this can be understood in terms of increased inertia. However, the effective higher mass, μ in Eq. (26), is not attributable to the external field. Since the internal Coulomb field drives the electron towards relativistic speeds, also this contributes to an increased inertia which, in effect, renders the external field experienced by the electron weaker: $A \to A_{\text{eff}}$. The proper Dirac Hamiltonian, Eq. (2), with the interaction given in terms of the operator $c\boldsymbol{\alpha}$, accounts for this increase of inertia; the semirelativistic formulation, Eq. (16), does not. Specifically, the nonrelativistic dipole interaction term in Eq. (16) features the rest mass m, with no increased inertia and, thus, no effective reduction in field strength.

IV. CONCLUSIONS

We studied the role of relativistic corrections in photoionization of hydrogenlike ions by laser pulses. For hydrogen, the wavelengths ranged from the weakly ultraviolet region up to the onset of the optical region, while, in order to facilitate comparison, the field parameters were scaled appropriately with the nuclear charge for ions.

We took advantage of a semirelativistic approximation of the Dirac Hamiltonian to study the nature of the relativistic corrections—an approximation which combined a fully

relativistic spectrum with nonrelativistic interaction terms. While it was well known that the increased ionization potential of highly charged ions accounted for most of the relativistic shifts, we also identified how the increased inertia of the bound electron leads to an effective stabilization: The Coulomb field of highly charged nuclei accelerates the electron towards relativistic speeds, which, in turn, renders the external electric field of the laser weaker, in effect, than would be the case for a nonrelativistic electron.

ACKNOWLEDGMENTS

We would like to thank the authors of Ref. [27] for providing us with data for benchmarking our implementation. We also thank Sigma2—the National Infrastructure for High Performance Computing and Data Storage in Norway—for providing the resources necessary for implementing our calculations (Project No. NN9417K). Also, fruitful discussions with Prof. Eva Lindroth and Prof. Morten Førre are gratefully acknowledged.

[1] A. Di Piazza, C. Müller, K. Z. Hatsagortsyan, and C. H. Keitel, Rev. Mod. Phys. **84**, 1177 (2012).
[2] J. W. Braun, Q. Su, and R. Grobe, Phys. Rev. A **59**, 604 (1999).
[3] F. Fillion-Gourdeau, E. Lorin, and A. D. Bandrauk, Comput. Phys. Commun. **183**, 1403 (2012).
[4] I. A. Ivanov, Phys. Rev. A **91**, 043410 (2015).
[5] F. Fillion-Gourdeau, E. Lorin, and A. Bandrauk, J. Comput. Phys. **307**, 122 (2016).
[6] T. Kjellsson, S. Selstø, and E. Lindroth, Phys. Rev. A **95**, 043403 (2017).
[7] T. Kjellsson, M. Førre, A. S. Simonsen, S. Selstø, and E. Lindroth, Phys. Rev. A **96**, 023426 (2017).
[8] B. Hafizi, D. F. Gordon, and J. P. Palastro, Phys. Rev. Lett. **118**, 133201 (2017).
[9] T. K. Lindblom, M. Førre, E. Lindroth, and S. Selstø, Phys. Rev. Lett. **121**, 253202 (2018).
[10] D. A. Tumakov, D. A. Telnov, and G. Plunien, Eur. Phys. J. D **74**, 188 (2020).
[11] D. A. Telnov and S.-I. Chu, Phys. Rev. A **102**, 063109 (2020).
[12] D. A. Telnov and S.-I. Chu, Phys. Rev. A **104**, 023111 (2021).
[13] J. E. Vembe, E. A. B. Johnsen, and M. Førre, Phys. Rev. A **109**, 013107 (2024).
[14] F. Fillion-Gourdeau, S. MacLean, and R. Laflamme, Phys. Rev. A **95**, 042343 (2017).
[15] S. Blanes, F. Casas, J. Oteo, and J. Ros, Phys. Rep. **470**, 151 (2009).
[16] S. Selstø, E. Lindroth, and J. Bengtsson, Phys. Rev. A **79**, 043418 (2009).
[17] J. R. Vázquez de Aldana, N. J. Kylstra, L. Roso, P. L. Knight, A. Patel, and R. A. Worthington, Phys. Rev. A **64**, 013411 (2001).
[18] M. Førre and A. S. Simonsen, Phys. Rev. A **93**, 013423 (2016).
[19] A. S. Simonsen and M. Førre, Phys. Rev. A **93**, 063425 (2016).
[20] M. Førre and S. Selstø, Phys. Rev. A **101**, 063416 (2020).
[21] M. C. Suster, J. Derlikiewicz, K. Krajewska, F. C. Vélez, and J. Z. Kamiński, Phys. Rev. A **107**, 053112 (2023).
[22] M. C. Suster, J. Derlikiewicz, J. Z. Kamiński, and K. Krajewska, Opt. Express **32**, 6085 (2024).
[23] T. K. Lindblom, M. Førre, E. Lindroth, and S. Selstø, Phys. Rev. A **102**, 063108 (2020).
[24] M. Førre, Phys. Rev. A **99**, 053410 (2019).
[25] T. Kjellsson Lindblom and S. Selstø, Phys. Rev. A **104**, 043102 (2021).
[26] M. Sonnleitner and S. M. Barnett, Phys. Rev. A **98**, 042106 (2018).
[27] I. V. Ivanova, V. M. Shabaev, D. A. Telnov, and A. Saenz, Phys. Rev. A **98**, 063402 (2018).
[28] L. L. Foldy and S. A. Wouthuysen, Phys. Rev. **78**, 29 (1950).
[29] L. B. Madsen and P. Lambropoulos, Phys. Rev. A **59**, 4574 (1999).
[30] Y. V. Vanne and A. Saenz, Phys. Rev. A **85**, 033411 (2012).
[31] C. deBoor, *A Practical Guide to Splines* (Springer, New York, 1978).
[32] C. F. Fischer and O. Zatsarinny, Comput. Phys. Commun. **180**, 879 (2009).
[33] Y. Saad, SIAM J. Numer. Anal. **29**, 209 (1992).